Structural Engineering and Mechanics, Vol. 38, No. 4 (2011) 459-477
DOI: http://dx.doi.org/10.12989/sem.2011.38.4.459

Flexural behavior of concrete beams reinforced with aramid fiber reinforced polymer (AFRP) bars

Min Sook Kim[1a], Young Hak Lee*[1], Heecheul Kim[1b], Andrew Scanlon[2b] and Junbok Lee[1c]

[1]*Department of Architectural Engineering, Kyung Hee University, Yongin, Korea*
[2]*Department of Civil Engineering, The Pennsylvania State University, University Park, USA*

(Received April 28, 2010, Accepted February 22, 2011)

Abstract. Due to the low elastic modulus of FRP, concrete members reinforced with FRP rebars show greater deflections than members reinforced with steel rebars. Deflection is one of the important factors to consider the serviceability of horizontal members. In this study flexural test of AFRP reinforced concrete beams was performed considering reinforcement ratio and compressive strength as parameters. The test results indicated that flexural capacity and stiffness increase in proportion to the reinforcement ratio. The test results were compared with existing proposed equations for the effective moment of inertia including ACI 440. The most of the proposed equations were found to over-estimate the effective moment of inertia while the equation proposed by Bischoff and Scanlon (2007) most accurately predicted the values obtained through actual testing.

Keywords: AFRP rebar; beam; reinforcement ratio; concrete compressive strength; deflection; effective moment of inertia; serviceability.

1. Introduction

Previous studies have shown that FRP reinforced concrete is not fully conducive to the use of existing design methods intended for steel reinforced concrete because of the difference in the material properties of steel rebar and FRP rebar (ACI committee 440 2006, Benmokrane *et al.* 1996, Bischoff and Scanlon 2007, Toutanji and Saafi 2000, Yost *et al*. 2003). While steel reinforced concrete beams generally have reinforcement ratio of 1% or higher, FRP reinforced beams are designed to have reinforcement ratio of less than 1% due to the high tensile strength and low elastic modulus of FRP rebar. Design requirements provided by ACI 318-08 (ACI committee 318 2008) have been found to underestimate deflections in beams with reinforcement ratio of less than 1% by assuming excessively large degree of stiffness (Bischoff and Scanlon 2007). In order to predict effective moment of inertia of FRP reinforced concrete beams, many researchers have proposed modified forms of equations for FRP reinforced concrete beams, which have been calibrated the

*Corresponding author, Assistant Professor, E-mail: leeyh@khu.ac.kr
[a]Ph.D. Candidate
[b]Professor
[c]Associate Professor

existing equation for typical steel reinforced concrete beams by reflecting experiment results of FRP reinforced concrete beams (Benmokrane *et al*. 1996, Toutanji and Saafi 2000, Yost *et al*. 2003, ACI committee 440 2006, Sarkar and Menon 2009, Lu *et al.* 2010, Zanuy 2010). However, these studies take a statistical and empirical approach based on a limited range of data; hence, they reveal their limitations when applied under a broader range of conditions, including FRP rebar type and load condition. Bischoff and Scanlon proposed an equation for calculating the effective moment of inertia that reflects not only the bond properties and mechanical characteristics of FRP rebar but also the tensile contribution of concrete after the cracking stage (Bischoff and Scanlon 2007). The purpose of this study is to examine the validities of the equations for the effective moment of inertia proposed by Bischoff and Scanlon and others, including the current ACI code, by comparing and analyzing them with the test results performed herein. Equations selected for the comparative analysis in this paper are those taken from Benmokrane *et al.* (1996), Toutanji and Saafi (2000), Yost *et al.* (2003), and ACI 440.1R (2006) as well as Bischoff and Scanlon (2007).

2. Test program

The test aims to evaluate the flexural behavior of beams with various compressive strengths and reinforcement ratios. For the latter, seven specimens with various ratios of AFRP reinforcement were manufactured using the balanced reinforcement ratio of Eq. (1), taken from ACI 440.1R-06, as the criterion for determining whether a specimen was under-reinforced, balanced-reinforced, or over-reinforced. Two additional specimens of steel reinforced concrete were manufactured to compare the behavior of AFRP reinforced concrete beams with that of typical steel reinforced concrete beams. The details of the specimens are presented in Table 1.

Table 1 Details of tested beams

Beam No.	Rebar	Concrete strength (MPa)	Reinforced ratio		Design of reinforcement
			ρ_{fb} (%)	ρ_{design} (%)	
A2D8-27	AFRP	27	0.16	0.14	Balanced
A4D8-27				0.28	Over
A6D8-27				0.42	Over
A2D8-45		45	0.23	0.14	Under
A3D8-45				0.21	Balanced
A3D10-45				0.33	Over
A4D10-45				0.44	Over
S2D10-27	Steel	27	1.79	0.22	Under
S4D10-27				0.44	Under

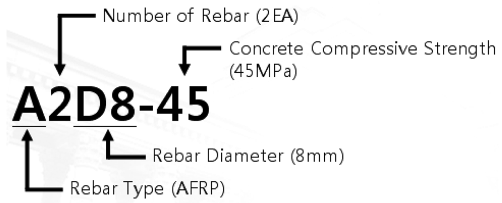

Table 2 Mechanical properties of rebars

Bar Type	Diameter (mm)	Area of cross section (mm^2)	Nominal ultimate strength (MPa)	Elastic modulus (GPa)
AFRP	8	50	1414.7	61.7
	10	79		
Steel	10	79	489	200

$$\rho_{fb} = 0.85\beta_1 \frac{f_c'}{f_{fu}} \frac{E_f \varepsilon_{cu}}{E_f \varepsilon_{cu} + f_{fu}} \tag{1}$$

where, E_f = design modulus of elasticity of FRP

f_c' = compressive strength of concrete

f_{fu} = design tensile strength of FRP

β_1 = rectangular stress block factor for depth of compression zone

ε_{cu} = ultimate strain in concrete

2.1 Materials

For the FRP reinforced specimens, 8 mm and 10 mm diameters of AFRP rebars were used. For the specimens reinforced the steel reinforcement, Steel bars of 10 mm diameter with the tensile strength of 400 MPa were used as rebars and stirrups. The AFRP rebars were manufactured with Aramid fiber and epoxy resin; the ratio of the fiber area to the total cross section area was 75%. The surface of the AFRP rebars was covered with spiral ribs and sand coating to enhance bond strength; the material test results for the AFRP rebars are given in Table 2. In order to measure the compressive strength of the concrete, twelve Ø150 mm × 300 mm were manufactured and tested on 28 days. As results, average compressive strengths were 25.1 MPa and 45.4 MPa, respectively.

2.2 Specimens

Specimens were designed to have a dimension of 200 mm × 400 mm × 3980 mm with a cover of 40 mm. To induce flexural failure while preventing shear failure, all specimens were reinforced at the shear zone with Ø 10 stirrups at 150 mm intervals. To prevent crushing caused by an overlap between stirrup and loading point, stirrups at the central loading point were placed at 300 mm intervals. Details of the specimens are illustrated in Fig. 1.

As shown in Fig. 1, specimens were subjected to third point loading in a simply supported condition. The distance from support to loading point was 1,290 mm (shear span ratio = 3.6), and the distance between the two loading points was 600 mm. Load was applied by affixing a oil jack of 1,000 kN capacity to the upper frame; load measurements were taken using a load cell installed at the bottom of the oil jack. For deflection, the average value of two LVDTs installed at the upper and lower centers of each specimen was used in this paper. Strains of concrete and AFRP rebar were obtained from the strain gages attached to the surface of the concrete and the middle of the AFRP rebar during the tests.

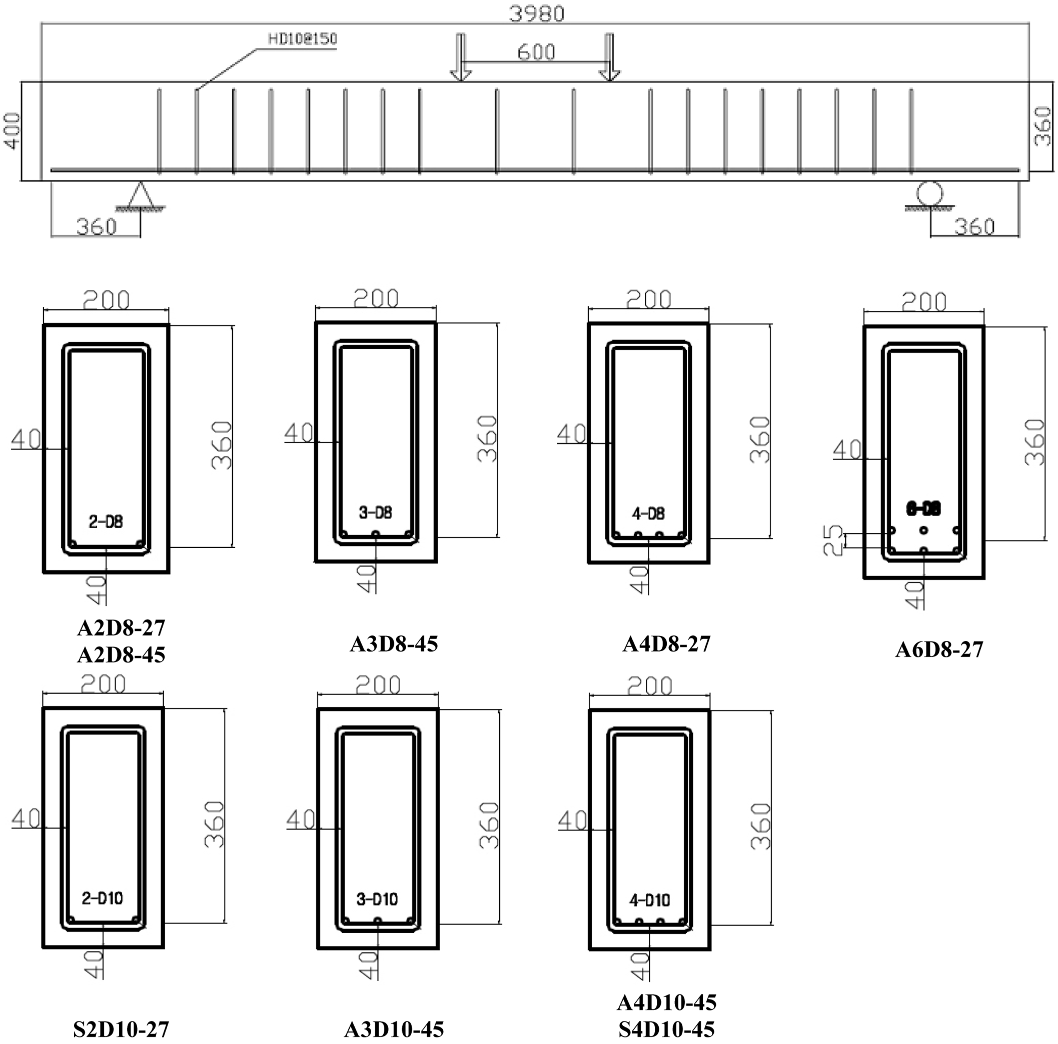

Fig. 1 Details of typical beams

3. Experimental results and discussion

3.1 Cracking behavior

Fig. 2 shows the crack pattern caused by maximum loading for each specimen. All AFRP reinforced specimens showed flexural cracking in the central region during initial loading. Thereafter, as the load was increased, cracking propagated out of the pure bending zone, and cracks that began in the concrete tensile zone began progressing toward the compressive zone, eventually leading to yield or failure. Also, in specimens reinforced with AFRP rebar, cracks were spaced closer together than in specimens reinforced with steel rebar. This is because the tension stiffening effect was sustained for a longer period in the AFRP reinforced specimens than in the steel

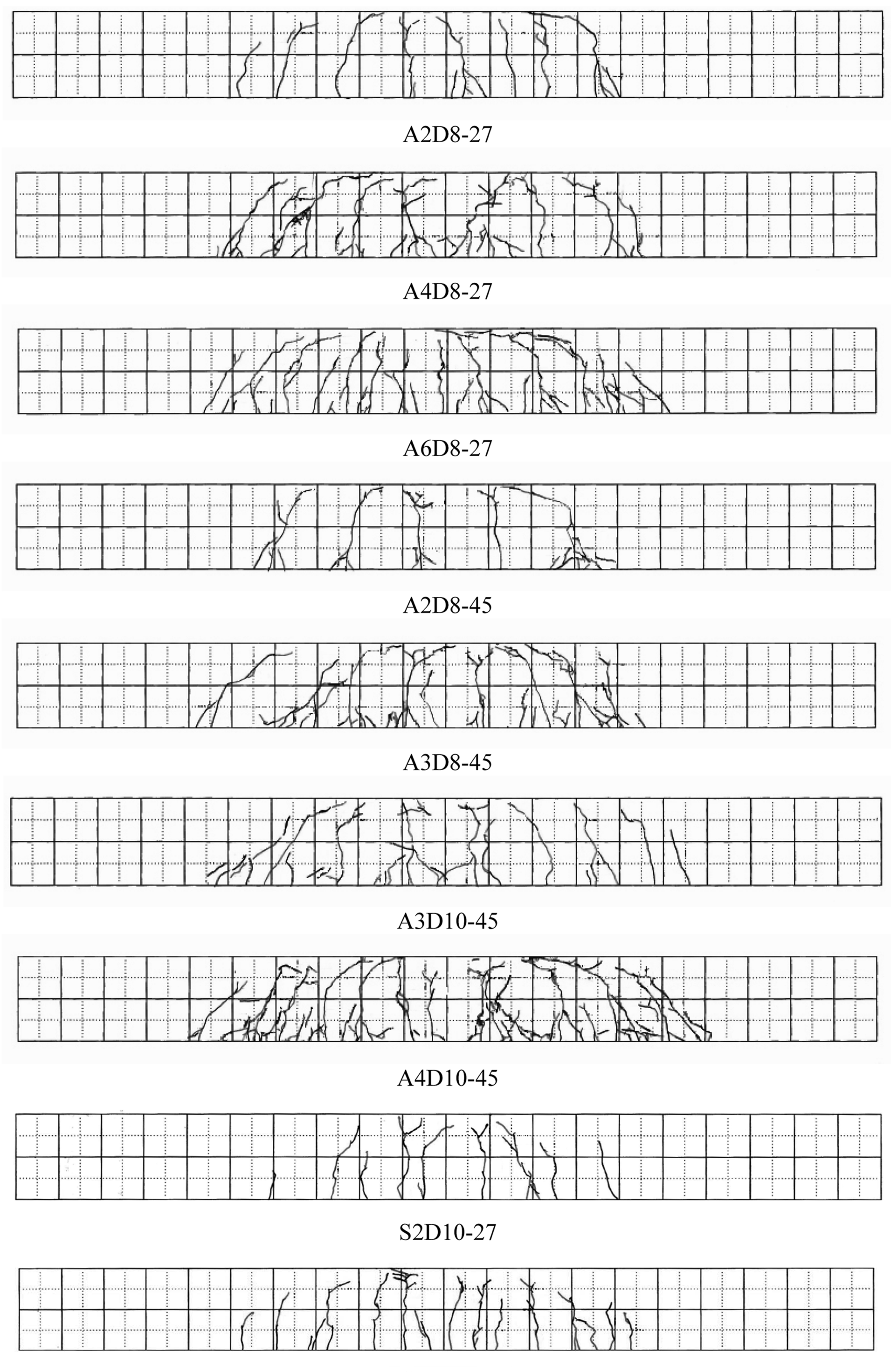

Fig. 2 Distribution of cracks on specimens

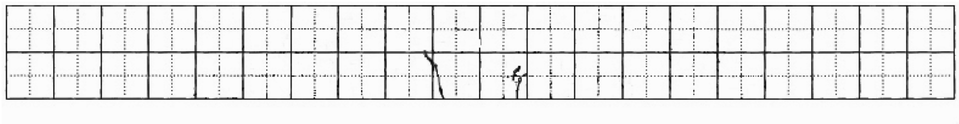

(a) $0.2P_u$

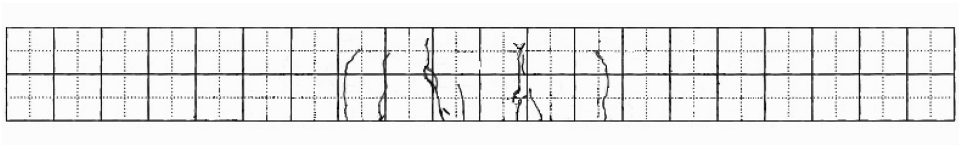

(b) $0.4P_u$

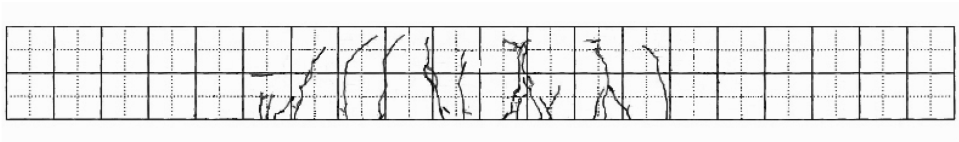

(c) $0.6P_u$

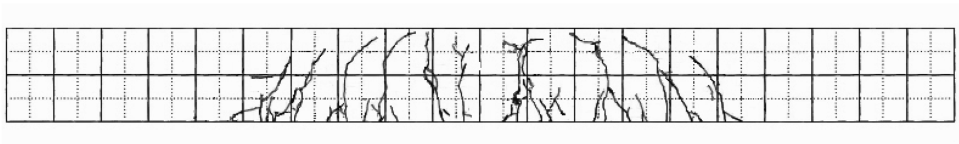

(d) $0.8P_u$

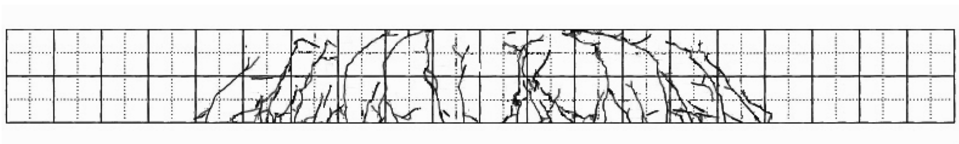

(e) P_u

Fig. 3 Typical crack pattern in AFRP reinforced beam at various loading stages: (a) $0.2P_u$, (b) $0.4P_u$, (c) $0.6P_u$, (d) $0.8P_u$, (e) P_u

reinforced specimens, due to the lower bond stress transferred from the AFRP to the concrete (Bischoff 2007, Nayal and Rasheed 2006). After initial cracking, cracks progressed faster in the AFRP reinforced specimens than in the steel reinforced specimens, because the low elastic modulus of the FRP rebar resulted in a decrease in stiffness after cracking. Fig. 3 shows the progression of cracks caused by increased loading in specimen A4D10-45. Initial cracks appeared within the pure bending zone at the center of the specimen, then dispersed outward from the pure bending zone. Thereafter, secondary cracks appeared between the existing cracks, showing a gradual progression toward shear cracking.

3.2 Modes of failure

According to the test results, FRP reinforced specimens exhibited two modes of failure, caused by either FRP rupture or concrete crushing. Fig. 4 illustrates these two failure modes.

As reported in the ACI 440 report as well as in previous studies, under-reinforced specimen

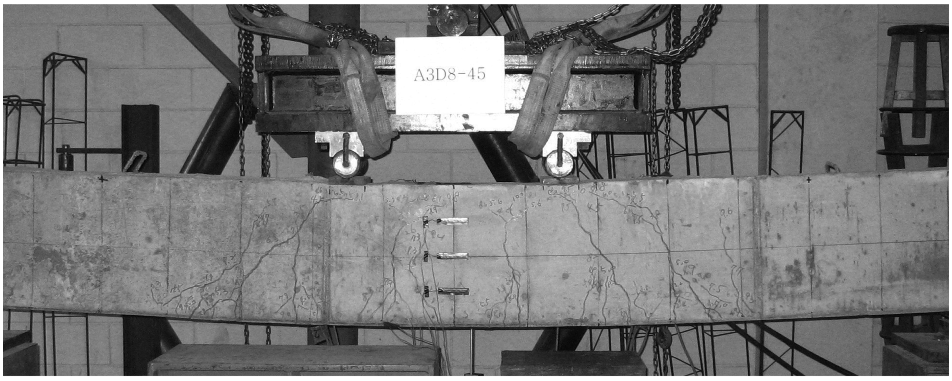

(a) FRP rupture failure mode

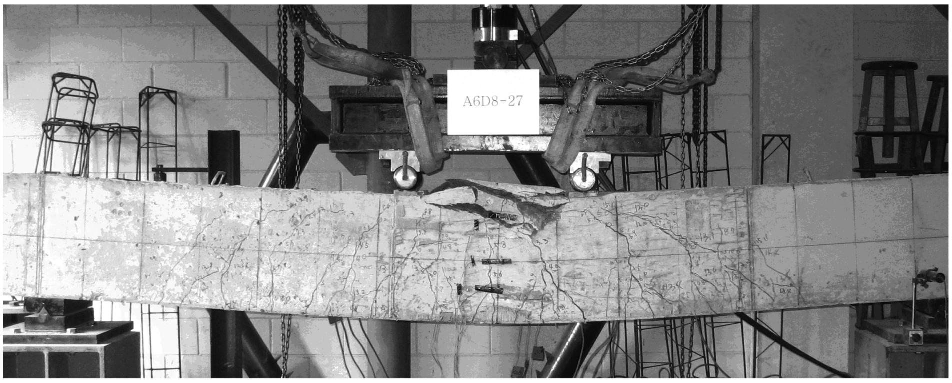

(b) Concrete crushing failure mode

Fig. 4 Typical failure modes of beams reinforced with AFRP bars

A2D8-45 and balanced-reinforced specimens A2D8-27 and A3D8-45 showed brittle failure caused by FRP rupturing after the maximum loads. No cracks appeared in the compressive zone of the concrete before the specimen reached around the maximum load. This is because the AFRP rebar exceeded its ultimate tensile strain before the concrete compressive zone reached the ultimate strain. In this case, the brittle properties of the FRP rebar had a direct effect on the occurrence of brittle failure. By contrast, over-reinforced specimens A4D8-27, A6D8-27, A3D10-45, and A4D10-45 showed rapid declines in load after the maximum loadings, while simultaneously displaying cracks in the compressive zone of the concrete. However, their behaviors thereafter showed that they maintained certain degree of resisting forces. Whereas both modes of failure seen in the AFRP reinforced specimens showed the brittle failure, the steel reinforced specimens exhibited ductile behavior after the maximum loading. While brittle failure was more prominent in the AFRP reinforced specimens than in the steel reinforced specimens, limited ductile behavior—i.e., the maintenance of some resisting force after decreased load—was more clearly observable in the cases of failure caused by concrete crushing.

3.3 Load-deflection relationship

Fig. 5 shows the load-deflection relationship of steel reinforced concrete beams and AFRP

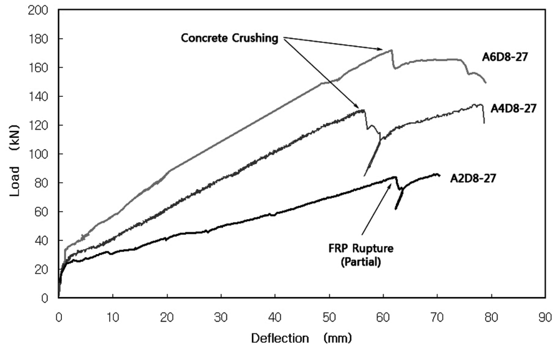

(a) AFRP, $f_{c'} = 27$MPa

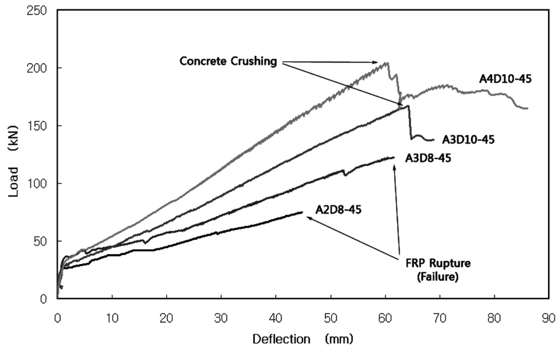

(b) AFRP, $f_{c'} = 45$MPa

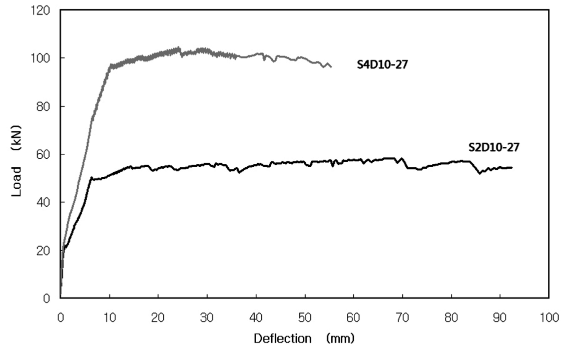

(c) Steel, $f_{c'} = 27$MPa

Fig. 5 Load-deflection relations

reinforced concrete beams with the various reinforcement ratios. Regardless of the reinforcement ratio, all specimens showed declines in stiffness as soon as cracking began, and exhibited linear behavior until they reached the maximum load, or yield load. In the over-reinforced specimens, load reduction occurred by a large margin after the occurrence of concrete crushing at maximum load, but a certain degree of resisting force was maintained. Contrarily, the under-reinforced specimens and the balanced-reinforced specimens showed the simultaneous occurrence of FRP rupturing and brittle failure under maximum load. The steel reinforced specimens maintained resisting force after yield load, with only deflection tending to increase.

As shown in Fig. 5, all specimens, regardless of the compressive strength of the concrete, exhibited increase in stiffness and maximum load as their reinforcement ratios increased. AFRP reinforced specimens tended to have lower stiffness than steel reinforced specimens, due to the low elastic modulus of the AFRP rebar used as reinforcement. This signifies that, under the same load, AFRP reinforced specimens undergo greater deflection than steel reinforced specimens.

3.4 Load-strain relationship

Fig. 6 illustrates the strain relationship of the bottom bar and the concrete compressive face (middle of span) relative to increased load in over-reinforced specimens A6D8-27 and A4D10-45, which have the same reinforcement ratio. Since the same amount of rebar was used in A4D10-45 and A6D8-27, both showed identical stiffness in the tensile zone; however, stiffness in the concrete

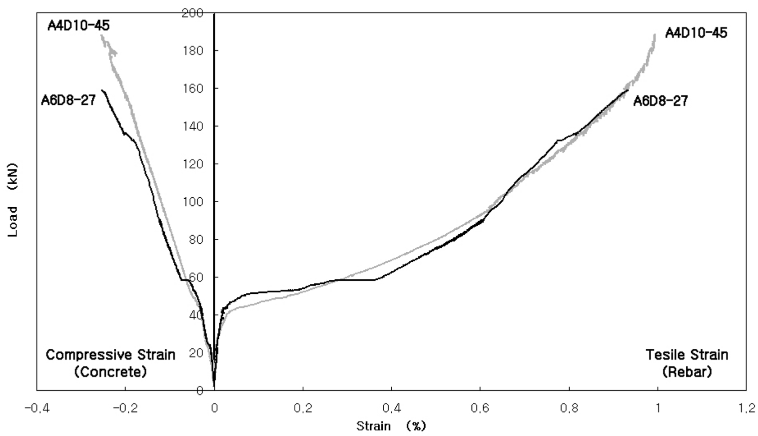

Fig. 6 Load-strain relations

compressive zone is greater in specimen A4D10-45. Also, based on the fact that A4D10-45 demonstrates greater maximum load than A6D8-27, it can be deduced that the compressive strength of concrete has a greater impact on the enhancement of resisting force when the beam in question has been over-reinforced.

4. Comparison of predictions and experimental results

4.1 Cracking and ultimate moment

The test results and the cracking moment and ultimate moment calculated using the equation in ACI 440.1R-06 are summarized in Table 3. By analyzing the data on load-deflection and load-strain relationships, the point at which initial stiffness begins to change was regarded as the load which causes initial structural cracking. The cracking moment M_{cr} thus measured was then compared with the values derived from Eq. (2) proposed in ACI 440.1R-06.

$$M_{cr} = \frac{2f_r I_g}{h} \tag{2}$$

where, $f_r = 0.62\sqrt{f_c'}$ (concrete rupture modulus)

h = overall height of beam

$I_g = \dfrac{bh^3}{12}$ (gross moment of inertia)

b = beam width

The cracking moment M_{cr} calculated using the ACI 440 equation showed a relatively large difference from the test results. The range of the calculation ratio to the experiment is from 0.74 to 1.22. Previous studies have proven that this difference results from the presence of shrinkage restraint stress, which reduces the cracking moment according to the reinforcement ratio, and the diverse modulus of rupture resulting from varying mixture densities (ACI committee 435 1995,

Table 3 Cracking and ultimate moment capacity

	M_{cr} (kN·m)		$\frac{M_{cr\ theo}}{M_{cr\ \exp}}$	M_u (kN·m)		$\frac{M_{u\ theo}}{M_{u\ \exp}}$
	Theoretical	Experimental		Theoretical	Experimental	
A2D8-27	16.6	15.7	1.06	50.0	54.1	0.93
A4D8-27		17.6	0.94	70.3	84.4	0.83
A6D8-27	18.5	22.3	0.74	83.3	110.9	0.75
A2D8-45	22.3	17.6	1.05	50.6	48.4	1.05
A3D8-45		23.1	0.97	75.9	78.9	0.96
A3D10-45		18.3	1.22	105.4	107.7	0.98
A4D10-45		22.6	0.99	119.4	121.3	0.98
S2D10-27	16.6	13.6	1.22	22.9	32.4	0.71
S4D10-27		15.3	1.08	54.2	62.8	0.86

Scanlon and Bischoff 2008). In FRP reinforced specimens, the low elastic modulus of the FRP rebar results in correspondingly low flexural stiffness, which in turn causes greater deflection than that of steel reinforced concrete. Therefore, when evaluating serviceability, it is reasonable to set the service load at 30% of the nominal performance level; at the same time, the accurate calculation of the cracking moment M_{cr} is an important factor to consider in predicting deflection (Bischoff 2007, Bischoff and Scanlon 2007, Rafi *et al*. 2008, Yost *et al*. 2003). As noted above, however, there was a relatively large difference between the values derived from ACI 440 equation and the test results; hence, M_{cr} measured from the test results was utilized for the calculation of deflection. To compare the ultimate moments calculated from ACI 440 equation with the values measured during testing, the ultimate moment M_u was calculated according to Eq. (3) using the maximum load P obtained through testing, and the nominal moment M_n was calculated as shown in Eq. (4), in accordance with ACI 440.1R-06.

$$M = \frac{P}{2} \times 1.29 \tag{3}$$

$$\begin{aligned} \rho_f > \rho_{fb}, \quad M_n &= \rho_f f_f \left(1 - 0.59\frac{\rho_f f_f}{f_c'}\right) b d^2 \\ \rho_f < \rho_{fb}, \quad M_n &= \rho_f f_f \left(d - \frac{\beta_1 c_b}{2}\right) \end{aligned} \tag{4}$$

where, c_b = distance from extreme compression fiber to neutral axis at balanced strain condition

d = effective depth of beam

$$f_f = \left(\sqrt{\frac{(E_f \varepsilon_{cu})^2}{4} + \frac{0.85\beta_1 f_c'}{\rho_f} E_f \varepsilon_{cu}} - 0.5 E_f \varepsilon_{cu}\right) \le f_{fu}$$

ρ_f = FRP reinforcement ratio

ρ_{fb} = FRP balanced reinforcement ratio

The ratio of the calculated ultimate moment to that obtained through testing was 0.93 on average, thus showing a relatively small margin of error. Thus, the equation for the ultimate moment proposed in ACI440.1R-06 can be said to predict the actual ultimate moment with relative accuracy.

4.2 Deflection

Because of the low elastic modulus of FRP, deflection is greater in FRP reinforced concrete than in steel reinforced concrete; thus, the serviceability of FRP reinforced beam should be considered as one of the important factors. FRP reinforced members have lower flexural stiffness; thus, whereas 60% of the nominal performance of typical steel reinforced concrete members is considered as the service load for the serviceability, only 30% is considered for the serviceability of FRP reinforced concrete members (Bischoff 2007, Bischoff and Scanlon 2007, Rafi *et al*. 2008, Yost *et al*. 2003). Therefore, in this study, deflection under service load was compared by applying $P_u/1.7$ as the service load for steel reinforced concrete and $0.3P_u$ as the service load for FRP reinforced concrete. The deflection of a beam under third point loading can be calculated as shown in Eq. (5).

$$\delta = \frac{M}{24E_cI_e}(3L^2 - 4a^2) \tag{5}$$

where, M = moment

E_c = Modulus of elasticity of concrete

I_e = effective moment of inertia

L = net span of the beam

a = shear span

When calculating deflection, the effective moment of inertia I_e is an important factor for predicting deflection. The Eq. (6) proposed by Branson has been widely used to calculate the effective moment of inertia in typical steel reinforced concrete members (ACI Committee 318 2005, Branson 1965)

$$I_e = \left(\frac{M_{cr}}{M_a}\right)^3 I_g + \left[1 - \left(\frac{M_{cr}}{M_a}\right)^3\right] I_{cr} \le I_g \tag{6}$$

where, $I_{cr} = \frac{bd^3}{3}k^3 + n_f A_f d^2 (1-k)^2$

$k = \sqrt{(\rho_f n_f)^2 + 2\rho_f n_f} - \rho_f n_f$

M_a = applied moment

M_{cr}= cracking moment

A_f = area of FRP reinforcement

n_f= ratio of modulus of elasticity of FRP bars to modulus of elasticity of concrete

While Branson's equation has been shown to take adequate tension stiffening into account when applied to members with a reinforcement ratio of 1% or higher—i.e., members for which the ratio of the gross moment of inertia to the cracked transformed moment of inertia (I_g/I_{cr}) is 2-3—it tends to over-estimate the tension stiffening effect in members with a reinforcement ratio of under 1% ($I_g/I_{cr} \ge 4$), such as FRP reinforced concrete. In the specimens used for the current study, I_g/I_{cr} was highest at 46.8 when the reinforcement ratio was 4.4. Fig. 7 compares the results of testing specimen A3D8-45, which has an I_g/I_{cr} value of 31.9, with the values derived from Branson's

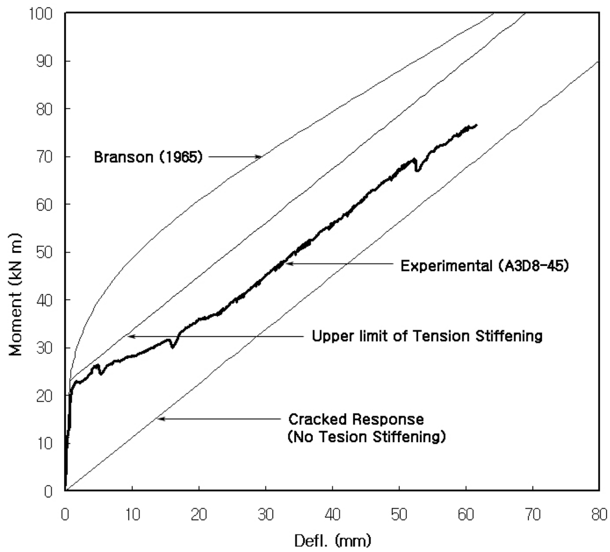

Fig. 7 Branson and experimental responses for A3D8-45 (I_g/I_{cr} = 31.9)

equation. As the figure shows, whereas the response of the specimen must fall between the maximum tension stiffening value and the member's crack response value (I_{cr}), the values obtained from Branson's equation falls outside of the limits of maximum stiffening after initial cracking load. This indicates that, when I_g/I_{cr} has a large value, Branson's equation over-estimates tension stiffening and thus under-predicts deflection. Previous studies have also demonstrated that the progression of the steel reinforced concrete model, which changes non-linearly due to tension stiffening as it progresses from the gross section to the cracked transformed section, is not appropriate for FRP reinforced concrete models (Bischoff 2007, Nayal and Rasheed 2006, Yost *et al.* 2003).

Benmokrane *et al.* (1996) conducted flexural testing on GRFP-reinforced beams using the reinforcement ratio as the variable, and demonstrated that, unlike steel reinforced concrete beams, FRP reinforced beams exhibited numerous wide cracks past the point of cracking load. Based on this result, the authors argued that Branson's equation over-estimates the effective moment of inertia in FRP reinforced beams. Accordingly, they proposed Eq. (7) for the effective moment of inertia, which maintains the form of Branson's equation while applying a reduction factor to the gross section and the cracked transformed section on the basis of the test results.

$$I_e = \left(\frac{M_{cr}}{M_a}\right)^3 \frac{I_g}{7} + 0.84\left[1 - \left(\frac{M_{cr}}{M_a}\right)^3\right] I_{cr} \le I_g \tag{7}$$

Comparing the test results from the current study with the values obtained using the equation proposed by Benmokrane *et al.* reveals a significant discrepancy: while the response curve of specimen A4D8-27 remains above the curve for the cracked transformed moment of inertia until the point of maximum load, as shown in Fig. 8, the values derived from the equation by Benmokrane *et al.* drop below the curve for the cracked transformed moment of inertia before reaching maximum load. The same phenomenon was observed in all specimens, whether reinforced with steel or FRP rebar, and the discrepancy between the two sets of values increased in proportion to the

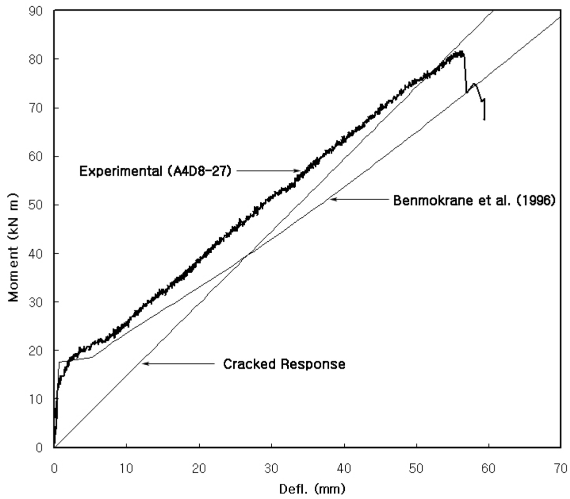

Fig. 8 Benmokrane *et al.* and experimental responses for A4D8-27

reinforcement ratio. Because the equation proposed by Benmokrane *et al.* is based only on data obtained under a limited set of conditions—i.e., the testing of GFRP reinforced beams using two reinforcement ratios as variables—it appears inadequate for making rational predictions when the range of rebar types and reinforcement ratios is broader.

Toutanji and Saafi (2000) judged that the equations proposed by Branson and other foregoing researchers over-estimates the effective moment of inertia by failing to take into account the unique characteristic of FRP, namely its low elastic modulus, and the resulting reinforcement ratio of under 1%. Accordingly, they conducted flexural testing on GFRP reinforced beams using the reinforcement ratio as the variable, and performed regression analysis on the test results and those reported previous researchers. Based on this analysis, the authors proposed Eq. (8), which adds a quotient equation that reflects the low elastic modulus and reinforcement ratio of FRP to the equation originally proposed by Branson.

$$I_e = \left(\frac{M_{cr}}{M_a}\right)^m I_g + \left[1 - \left(\frac{M_{cr}}{M_a}\right)^m\right] I_{cr} \le I_g \tag{8}$$

Where, $m = 6 - 10\frac{E_f}{E_s}\rho_f$ for $\frac{E_f}{E_s}\rho_f < 0.3$

$m = 3$ for $\frac{E_f}{E_s}\rho_f \ge 0.3$

E_s = modulus of elasticity of steel

The equation proposed by Toutanji and Saafi shows a non-linear relationship similar to that of Branson's equation. Nonetheless, it yielded more accurate predictions for specimens of varying reinforcement ratios than Branson's because it takes into consideration the effects of not only the modulus of elasticity but the reinforcement ratio as well. Fig. 9 is a comparison of the test results with the values obtained from Toutanji and Saafi's equation. It can be seen that the result values for

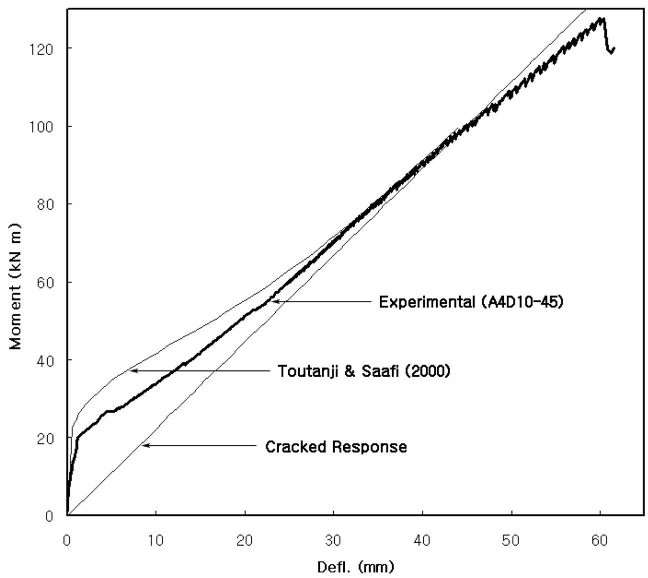

Fig. 9 Toutanji and Saafi and experimental responses for A4D10-45

specimen A4D10-45 predicts deflection with relative precision from around 60% of the ultimate load to the actual point of ultimate load, but under-predicts deflection under service load because it over-estimates stiffness after initial cracking load. This appears to be because the quotient m was originally proposed by carrying out regression analysis on specimens with a limited range of reinforcement ratios and elastic modulus; the equation is thus incapable of calculating an accurate effective moment of inertia for specimens that diverge from the previous testing environment or have a diverse set of variables.

Yost *et al*. (2003) noted that Branson's equation is adapted to the non-linear second moment of area in ordinary steel reinforced concrete, arguing that the equation is thus inappropriate for FRP reinforced beams due to differences in the tension stiffening effect. They thus proposed their own equation for the effective moment of inertia by adopting a calibration coefficient β, as shown in Eq. (9).

$$I_e = \left(\frac{M_{cr}}{M_a}\right)^3 \beta I_g + \left[1 - \left(\frac{M_{cr}}{M_a}\right)^3\right] I_{cr} \le I_g \tag{9}$$

Yost *et al*. observed that FRP reinforced beams exhibit a rapid decline in stiffness after cracking load and that the 0.5 value of α in Eq. (10), proposed in the existing ACI440.1R-03, accords significant weight to the gross moment of inertia. They used these observations to argue that the effect of the cracked transformed moment of inertia must be increased. They also argued that the impact of the reinforcement ratio must be reflected in the reduction factor and that the value of α needed to be smaller than 0.5, because the equation in ACI440.1R-03 over-estimates the effective moment of inertia in members with a low reinforcement ratio. On this basis, they conducted tests on 48 GFRP reinforced beams using the reinforcement ratio, compressive strength, and shear span ratio as variables. By performing linear regression analysis on the test results, they proposed an equation for the value of β as shown in Eq. (11), which applies the ratio of the reinforcement ratio to the balanced reinforcement ratio (ρ/ρ_b) to the value of α.

$$\beta = \alpha\left(\frac{E_f}{E_s}+1\right), \quad \alpha = 0.5 \tag{10}$$

$$\beta = \alpha\left(\frac{E_f}{E_s}+1\right), \quad \alpha = 0.064\left(\frac{\rho_f}{\rho_b}\right)+0.13 \tag{11}$$

For most of the specimens, the equation by Yost *et al*. yielded relatively more accurate predictions for deflection by estimating a lower initial stiffness than existing equations. However, when compared with the under-reinforced specimen A3D8-45, it was seen to under-predict deflection, as shown in Fig. 10. This appears to be the result of limiting the test conditions to GFRP reinforced beams that are over-reinforced—i.e., that have reinforcement ratios in excess of the balanced reinforcement ratio—in the process of proposing the equation. Due to the use of linear regression analysis, the equation thus reveals its limitations when used in conjunction with a more diverse range of reinforcement ratios.

The ACI 440 committee used an approach similar to that of Yost *et al*. to propose a equation that simplifies the reduction factor β based on data from existing studies, as shown in Eq. (12).

$$\beta = \frac{1}{5}\left(\frac{\rho_f}{\rho_s}\right) \le 1.0 \tag{12}$$

As illustrated in Fig. 10, comparison with the test results from the current study showed that the equation proposed in ACI440.1R-06 produced better predictions than the equation by Yost *et al*., but that it still tends to under-predict deflection.

The abovementioned equations use Branson's equation as the basic framework and extend its application to FRP reinforced members. By contrast, Bischoff and Scanlon do not define a reduction

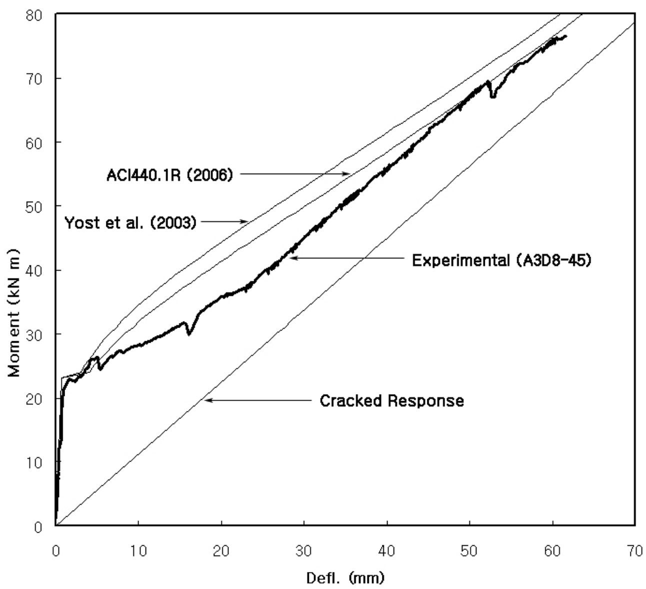

Fig. 10 Yost *et al*., ACI440.1R-06 and experimental responses for A3D8-45

factor β_d to mitigate the impact of the effective moment of I_e on the weighted average value of I_e, but instead weight flexibility over stiffness in considering tension stiffening with the idea of increasing the impact of low stiffness, i.e., I_{cr}, through the application of a serial combination for stiffness. The result is the proposed equation shown as Eq. (13) below (Bischoff and Scanlon 2007)

$$I_e = \frac{I_{cr}}{1-\left(\frac{M_{cr}}{M_a}\right)^2\left[1-\frac{I_{cr}}{I_g}\right]} \le I_g \tag{13}$$

This study examined the validity of the equations for the effective moment of inertia proposed by Branson, Benmokrane *et al*., Toutanji and Saafi, Yost *et al*., ACI440.1R-06, and Bischoff and Scanlon by calculating the corresponding deflection using Eq. (5) and comparing the obtained values with the actual test results. The comparison is summarized in Table 4 and Fig. 11.

Overall, Bischoff and Scanlon's equation was found to predict deflection with more accuracy than Branson's equation and others even without the application of the reduction factor β_d. The equations proposed by Benmokrane *et al*., Toutanji and Saafi, Yost et al., and ACI440.1R-06, which are all based on Branson's equation, addressed the over-estimation of the gross section stiffness (I_g) relative to the low stiffness of the FRP reinforced beam (I_{cr}) by carrying out quotient calibration through empirical statistical methods or by applying the reduction factor β_d. Nonetheless, they still tended to over-estimate stiffness in members with a low reinforcement ratio and thus under-predict deflection. Moreover, due to the limited FRP type, load, and point conditions used in testing, most of them revealed limitations when used to predict deflection under a more diverse set of conditions. By contrast, the equation proposed by Bischoff and Scanlon was seen to yield the most accurate predictions for deflection by using an approach that increases the impact of I_{cr} through the application of a series connection for stiffness, thus taking into consideration not only the bond characteristics and mechanical properties of FRP rebar but also the tensile contribution of concrete after the cracking stage.

Table 4 Comparison of deflections between experimental and theoretical

	$\delta_{service}$ (mm)						
	Experimental	Branson (1965)	Benmokrane (1996)	Toutanji and Saafi (2000)	Yost (2003)	Bischoff and Scanlon (2005)	ACI 440 (2006)
A2D8-27	1.3			0.54			
A4D8-27	4.4	1.16	6.91	1.55	3.46	4.23	3.16
A6D8-27	3.2	1.13	7.04	1.28	2.82	2.51	2.12
A2D8-45	0.8			0.41			
A3D8-45	1.3			0.62			
A3D10-45	11.8	3.60	12.57	7.09	8.61	11.84	8.70
A4D10-45	10.9	3.01	11.47	5.11	7.13	9.39	6.47
S2D10-27	2.1	0.94	4.47	1.05	2.83	1.85	0.94
S4D10-27	4.0	3.76	5.46	3.76	5.07	4.28	3.76

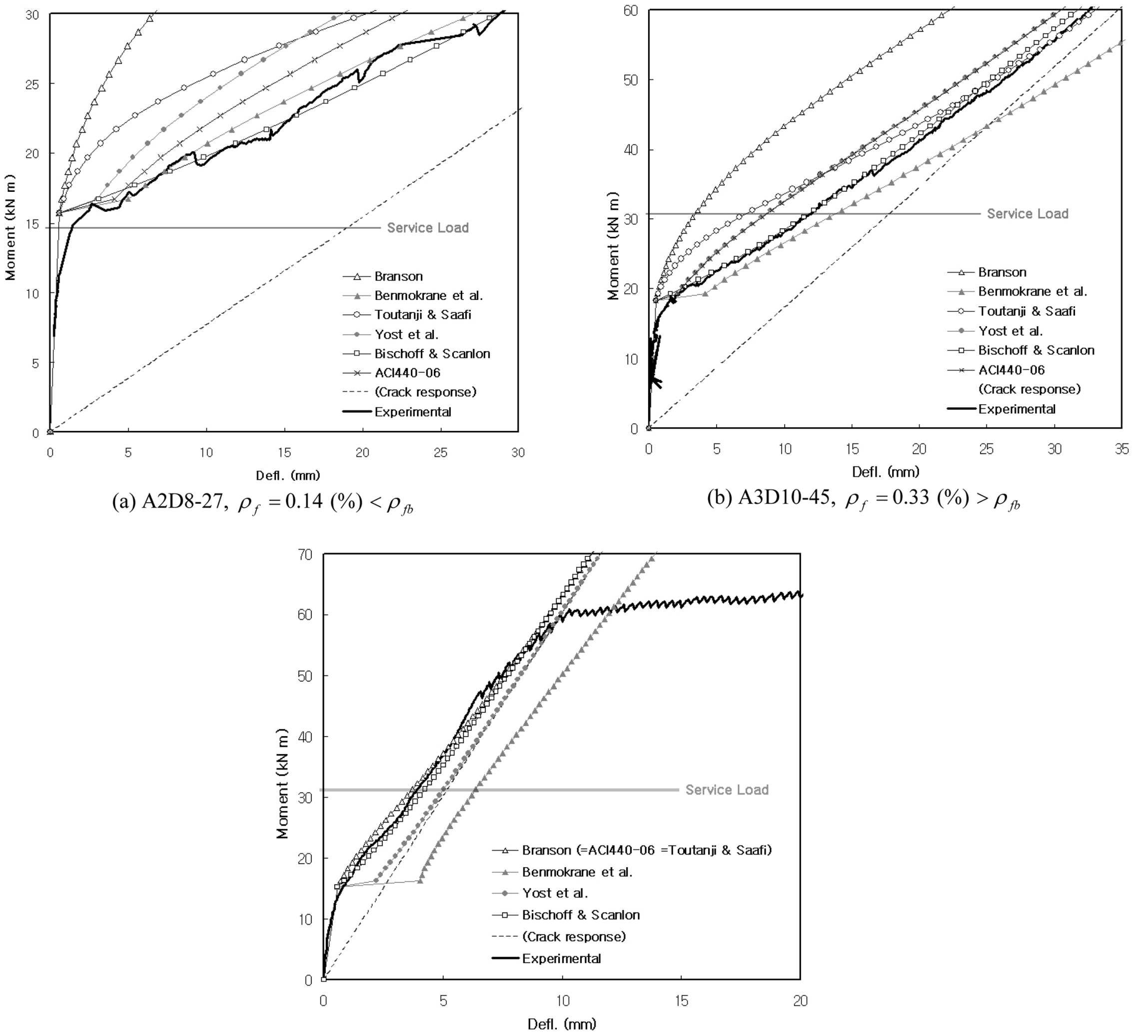

(a) A2D8-27, $\rho_f = 0.14$ (%) < ρ_{fb}

(b) A3D10-45, $\rho_f = 0.33$ (%) > ρ_{fb}

(c) S4D10-27, $\rho_f = 0.44$ (%) < ρ_{fb}

Fig. 11 Comparison between experimental data and proposed equations in moment-deflection relation

5. Conclusions

In this study, flexural testing was performed on concrete beams reinforced with AFRP rebar to compare their flexural performance relative to reinforcement ratio and compressive strength. The test results were then used to evaluate the feasibility of the equations for the effective moment of inertia proposed by previous researchers, including Bischoff and Scanlon. The conclusions thus reached are as follows:

1. In cases where the reinforcement ratio exceeded the balanced reinforcement ratio, higher compressive strength was found to enhance flexural performance in specimens with the same reinforcement ratio. Therefore, it can be concluded that compressive strength is a major factor for resisting force in over-reinforced concrete beams.

2. When the results of testing AFRP reinforced beams in the current study were compared with the values for deflection derived from the equations proposed by previous researchers, including Bischoff and Scanlon, the equations by Benmokrane *et al*., Toutanji and Saafi, Yost *et al*., and ACI440.1R-06, all based on Branson's equation, were found to over-estimate deflection, while Bischoff and Scanlon's equation tended to predict the test results with relative accuracy. This appears to be because Branson's equation and those based on it weight the stiffness of the gross section more than the stiffness of the cracked section, and because their use of empirical statistical methods limits the adaptability of their equations to a wide range of variables.
3. In predicting the ultimate moment, the values proposed in ACI 440.1R-06 predicted the test results with relative accuracy, by an average ratio of 0.93. However, in the case of the cracking moment, the calculated values produced a substantial margin of error. FRP reinforced concrete beams are greatly affected by the cracking moment due to their low service load; since this is an important factor in predicting deflection, further research is needed to devise a more rational equation for calculating the cracking moment.
4. The equation interpretation method proposed by Bischoff and Scanlon was found to predict the behavior of FRP reinforced concrete beams with the most accuracy. However, further experimental verification should be carried out using a more diversified set of conditions, including rebar type, reinforcement ratio, and load.

Acknowledgements

This work was supported by a grant from the Kyung Hee University in 2010 (KHU-20100627).

References

ACI Committee 318 (2005), *Building Code Requirements for Structural Concrete (ACI 318-05) and Commentary (318R-05)*, American Concrete Institute, Farmington Hills, Mich.

ACI Committee 440 (2006), *Guide for the Design and Construction of Concrete Reinforced with FRP Bars (ACI 440.1R-06)*, American Concrete Institute, Farmington Hills, Mich.

ACI Committee 435 (1995), *Control of Deflection in Concrete Structures (ACI 435R-95)*, American Concrete Institute, Farmington Hills, Mich.

Benmokrane, B., Chaallal, O. and Masmoudi, R. (1996), "Flexural response of concrete beams reinforced with FRP reinforcing bars", *ACI Mater. J.*, **91**(2), 46-55.

Bischoff, P.H. (2007), "Deflection calculation of FRP reinforced concrete beams based on modifications to the existing Branson equation", *J. Compos. Constr.*, **11**(1), 4-14.

Bischoff, P.H. and Scanlon, A. (2007), "Effective moment of inertia for calculating deflections of concrete members containing steel reinforcement and fiber-reinforced polymer reinforcement", *ACI Struct. J.*, **104**(1), 68-75.

Branson, D.E. (1965), *Instantaneous and Time-dependent Deflections of Simple and Continuous Reinforced Concrete Beams*, Alabama Highway Research Report, Report No. 7, Part 1.

Lu, W.Y., Hwang, S.J. and Lin, I.J. (2010), "Deflection prediction for reinforced concrete deep beams", *Comput. Concrete*, **7**(1), 1-16.

Nayal, R. and Rasheed, H.A. (2006), "Tension stiffening model for concrete beams reinforced with steel and FRP bars", *J. Mater. Civil Eng.*, **18**(6), 831-841.

Rafi, M.M., Nadjai, A., Ali, F. and Talamona, D. (2008), "Aspects of behavior of CFRP reinforced concrete beams in bending", *Constr. Buil. Mater.*, **22**, 277-285.

Sarkar, P., Govind, M. and Menon, D. (2009), "Estimation of short-term deflection in two-way RC slab", *Struct. Eng. Mech.*, **31**(2), 237-240.

Scanlon, A. and Bischoff, P.H. (2008), "Shrinkage restraint and loading history effects of deflections of flexural members", *ACI Struct. J.*, **105**(4), 498-506.

Toutanji, H.A. and Saafi, M. (2000), "Flexural behavior of concrete beams reinforced with glass fiber-reinforced polymer (GFRP) bars", *ACI Struct. J.*, **97**(5), 712-719.

Yost, J.R., Gross, S.P. and Dinehart, D.W. (2003), "Effective moment of inertia for glass fiber-reinforced polymer-reinforced concrete beams", *ACI Struct. J.*, **100**(6), 732-739.

Zanuy, C. (2010), "Investigating the negative tension stiffening effect of reinforced concrete", *Struct. Eng. Mech.,* **34**(2), 189-211.